Selective catalytic reduction of NO at low temperature using a (ethanol+ammonia) mixture over a Ag/Al2O3 + WO3/Cex-ZryO2 dual-bed catalytic system: Reactivity insight of WO3/Cex-ZryO2

Mathias Barreau, Xavier Courtois, Fabien Can

Catalysis Today 355 (2020) 375-384.
DOI: 10.1016/j.cattod.2019.08.019

Selective Catalytic Reduction of NO at low temperature using a (ethanol+ammonia) mixture over a Ag/Al_2O_3 + WO_3/Ce_x-Zr_yO_2 dual-bed catalytic system: reactivity insight of WO_3/Ce_x-Zr_yO_2.

Mathias Barreau [1], Xavier Courtois [1, *], Fabien Can [1, *]

[1] University of Poitiers, CNRS, UMR 7285 –Institut de Chimie des Milieux et Matériaux de Poitiers (IC2MP) – 4 rue Michel Brunet – TSA 51106 – 86073 Cedex 9, France

***** Corresponding authors: xavier.courtois@univ-poitiers.fr; fabien.can@univ-poitiers.fr

Abstract: The Selective Catalytic Reduction (SCR) is one of the most efficient process for NO_x removal from Diesel exhaust gas. However, the urea/NH_3-SCR process implemented in recent vehicles still suffers from a poor activity in the low temperature range (T < 250°C). One main reason is its dependency against the NO_2/NO_x ratio, limiting the expected fast-SCR reaction in this temperature range. Recently, we shown that the addition of ethanol to ammonia led to a significant increase of the activity of a Ag/Al_2O_3 catalyst in this low temperature range. Moreover, in a dual-bed configuration (Ag/Al_2O_3+WO_3/Ce_x-Zr_yO_2), a remarkable improvement was achieved at low temperature using only NO as NO_x. The present work aims to highlight the $DeNO_x$ chemistry encountered over the WO_3/Ce_x-Zr_yO_2 catalyst in a bifunctional (EtOH+NH_3) mixture. In addition to the fact that this process takes advantage of the low temperature NO_2 formation over the upstream Ag/Al_2O_3 catalyst, this work also puts in evidenced unexpected interactions between NO_2 and CH_3CHO (resulting from ethanol oxidation over Ag/Al_2O_3) thus leading to NO emission.

Keywords: $DeNO_x$; SCR; ethanol; ammonia; Ag/Al_2O_3; WO_3/Ce_x-Zr_yO_2

1. Introduction

Air pollution is now recognized as a major health risk. In 2013, the World Bank estimated that one in ten deaths in the world could be the result of air pollution. In addition to particulate matter (PM) and tropospheric ozone (O_3), nitrogen oxides (NO_x, *i.e.* NO and NO_2) are also considered as first-order pollutants. NO_x arise mainly from anthropogenic sources and result largely from combustion reactions. Vehicles, especially with Diesel engines, play a major concern in these emissions (39 % in 2013) [1].

Consequently more and more drastic legislations were adopted to limit the emission of air pollutants. To reach the recent Euro 6 standard about the NO_x emission limitations, manufacturers implement a dedicated catalytic system. Two main processes are commonly envisaged: the NO_x storage reduction (NSR) process [2,3] and the selective catalytic reduction (SCR) process [4]. Currently, the SCR process is the most commonly used system. In this case, an aqueous urea solution (AdBlue®) is directly injected into the exhaust pipe [5]. Urea is then decomposed into ammonia and reacts which NO_x leading to dinitrogen formation, according to the so-called "standard-SCR" reaction (1):

$$2\ NH_3 + 2\ NO + ½\ O_2 \rightarrow 2\ N_2 + 3\ H_2O \qquad (1)$$

However, in standard-SCR condition, the activity at low temperatures (T < 250°C) appears limited, which induces significant NO_x emissions during the cold start of the vehicles. A $DeNO_x$ improvement is obtained by a previous oxidation of NO to NO_2 in order to obtain an optimal NO_2/NO_x ratio of 0.5. The corresponding NO_x reduction stoichiometry is known as the "fast-SCR" reaction (2) [6]:

$$2\ NH_3 + NO + NO_2 \rightarrow 2\ N_2 + 3\ H_2O \qquad (2)$$

Conventional NH_3-SCR catalysts are made of oxide-based materials consisting of V_2O_5-WO_3-TiO_2 [7]. However, because of the possibility of vanadia sublimation [8,9], extensive efforts were made to develop vanadium free catalysts for mobile sources. Supported transition metal or ceria-based oxides such as $Fe_2O_3/WO_3/ZrO_2$ [10], MnO_x-CeO_2 [11], Nb-MnO_x [12] or $WO_3/Ce_xZr_{1-x}O_2$ [13,14] were proposed. Regarding $WO_3/Ce_xZr_{1-x}O_2$, tungsten addition was found to enhance the NO_x removal efficiency through the increase of the surface acidity and NH_3 adsorption properties [15]. Metal exchanged zeolites were also reported as highly active materials. Zeolites are generally promoted by transition metals, such as iron or copper and should offer small pore size to assure a suitable thermal stability [5,16,17]. Impressive $DeNO_x$ efficiencies were reported for these materials which remain however strongly dependant to the NO_2/NO_x inlet ratio.

In the exhaust pipe, the Diesel Oxidation Catalyst (DOC), originally dedicated to the treatment of carbon monoxide (CO) and unburned hydrocarbons (HC), is usually placed upstream the SCR catalyst to also partially oxidizes NO into NO_2 [18]. Unfortunately, this catalyst also exhibits kinetic limitation at low temperature, which limits the NO_2 emission and consequently impacts the efficiency of the NH_3-SCR process. As a result, new approaches are explored to avoid the DOC dependency, by developing catalytic systems more efficient at low temperatures (T < 250°C) in NO rich media.

Among the large choice of available reducing agent (unburned hydrocarbons, urea, ammonia, hydrogen… [19,20]), oxygenated HC like ethanol (EtOH), acetone or propanol [21] were also mentioned as attractive reductants. Supported silver materials, mainly Ag/Al_2O_3 catalysts, were reported as particularly active for this EtOH-SCR process [22–25]. It allows high $DeNO_x$

performances using a relatively safe and low-cost reductant. The EtOH-SCR mechanism involves numerous reactions [24]. The admitted reaction pathway is based on the ethanol oxidation into acetaldehyde, which then reacts with NO_x to form nitromethane (CH_3NO_2). Finally, nitromethane is decomposed into intermediate N-containing species such as HNCO or NH_3, reactive towards NO_x reduction into nitrogen. An important characteristic of this system is the ability of the Ag/Al_2O_3 catalyst to oxidize NO into NO_2, even at low temperature, concomitant with the ethanol dehydrogenation into acetaldehyde [22,26]. Unfortunately, EtOH-SCR process still suffers from a relatively poor $DeNO_x$ activity at T < 250°C, linked to the rate limiting step of nitromethane route formation [27,28].

In a recent work [29], we reported that co-feeding of ethanol and ammonia ((EtOH+NH_3)-SCR) over a Ag/Al_2O_3 catalyst was a promising way to enhance the $DeNO_x$ efficiency at low temperature (175 – 250°C), while avoiding NO_2 and DOC dependencies. (EtOH+NH_3)-SCR over Ag/Al_2O_3 catalyst had superior NO_x reduction efficiency than both NH_3-SCR and EtOH-SCR performed on the same sample in the 175 - 500°C temperature range. This synergetic effect observed at low temperature was explained by the activation of three different $DeNO_x$ pathways: (i) the original EtOH-SCR, (ii) the NH_3-SCR process, activated by NO_2 formed during EtOH-SCR (fast-SCR condition); and (iii) mainly by the H_2-assisted NH_3-SCR [30], occurring thanks to the H^* species provided by the ethanol dehydrogenation into acetaldehyde over the silver supported catalyst.

Even though a significant $DeNO_x$ enhancement was obtained by ammonia co-feeding in EtOH-SCR over Ag/Al_2O_3 catalyst, the outlet exhaust gas still contained residual ammonia and NO_x. Interestingly, NO_2 composed a high proportion of the remaining NO_x in the 175 – 300°C temperature range. The composition of the outlet exhaust gas being close to the fast-SCR condition, the addition of a conventional NH_3-SCR catalyst (WO_3/Ce_x-Zr_yO_2) downstream the EtOH-SCR catalyst was thus implemented. The $DeNO_x$ efficiency at low temperature was improved with ~~a~~ NO_x conversion between 46 and 95 % in the 175 – 250°C temperature range while only NO was injected as NO_x in the feed stream. This high $DeNO_x$ efficiency was then very similar to that recorded over NH_3-SCR materials in the most favourable fast-SCR condition.

The $WO_3/Ce_xZr_{1-x}O_2$ catalyst was selected as NH_3-SCR material because it appeared active with various NO_2/NO_x inlet ratios and it could act as an Ammonia Slip Oxidation Catalyst (ASC) to avoid ammonia release with a high selectivity towards N_2 [13]. We recently compared $WO_3/Ce_xZr_{1-x}O_2$ and exchanged Cu–FER as NH_3-SCR catalyst in the dual-bed configuration [31]. Compared to $WO_3/Ce_xZr_{1-x}O_2$, Cu-FER catalyst exhibited similar standard NH_3-SCR behaviour and promising higher fast-SCR activity at low temperature. Unfortunately, in the dual-bed configuration, the Cu-FER sample led to a lower $DeNO_x$ efficiency than $WO_3/Ce_xZr_{1-x}O_2$, despite higher ammonia conversion rates. Then, the Cu exchanged zeolite exhibited a less attractive use of ammonia compared to $WO_3/Ce_xZr_{1-x}O_2$.

In the present work, the Ag/Al_2O_3 + WO_3/Ce_x-Zr_yO_2 dual-bed reactivity was investigated with the aim to have a better understanding of the $WO_3/Ce_xZr_{1-x}O_2$ catalytic behaviour, especially toward the reactivity of carbon and nitrogen compounds.

2. Materials and methods

2.1. Catalysts preparation

Ag/Al_2O_3 catalyst, dedicated to NO_x reduction by ethanol, was prepared by silver impregnation (from $AgNO_3$ salt, Sigma Aldrich) on alumina (provided by Axens, previously calcined 4 hours under air at 700°C) in order to obtain of 2_{wt}% Ag. This silver content was selected because it is commonly described as an optimal loading [32]. The preparation method, detailed in [29], was inspired by the work of Sato *et al*. [33] in which ethanol was used as impregnation solvent rather than water because it allows a better silver dispersion thus a better $DeNO_x$ activity. The catalyst was finally calcined under wet air (10 $_{vol}$% H_2O) at 700°C for 4 h (heating rate of 5°C min^{-1}) and it is denoted Ag/Al in this article.

6 $_{wt}$% $WO_3/Ce_xZr_{1-x}O_2$ catalyst (noted as WO_3/Ce-Zr), was selected as NH_3-SCR material. The method of preparation was inspired by a previous study [13]. First, ceria-zirconia support (40 $_{wt}$% of CeO_2, supplied by Solvay) was aged 4 hours under air at 700°C. After dissolution of the desired amount of ammonium metatungstate ($(NH_4)_{10}W_{12}O_{41}$, $5H_2O$) in water, this solution was added to the Ce_x-Zr_yO_2 support and maintained at 60°C under continuous stirring for 30 minutes. After a drying step at 120°C for 12 hours, the obtained solid was finally calcined 4 hours at 700°C in wet air, as well as the Ag/Al material.

2.2. Characterizations

N_2 physisorption.

N_2 physisorption experiments were conducted with a Tristar 3000 (Micromeritics). The sample was firstly degassed 2 hours under vacuum at 250°C. N_2 adsorption was then realized at -196°C and the specific surface areas were determined from the Brunauer-Emmett-Teller (BET) method in the 0.05 – 0.25 p/p^0 range. ***X-Ray Diffraction.*** X-Ray Diffraction (XRD) patterns were collected using an Empyrean diffractometer (PANalytical) operating in the θ-2θ mode, using the Cu Kα radiation (λ = 1.5418 Å). The patterns were recorded from 2θ=20 to 120° with a scanning step of 0.1°.

H_2-Temperature Programmed Reduction.

Temperature Programmed Reduction (TPR) experiments were carried out using a Micromeritics Autochem 2920 device, equipped with a thermal conductivity detector (TCD). The sample (between 100 and 200 mg) was placed in a U-shaped reactor between two layers of quartz wool. Prior to the TPR measurement, the sample was first treated under pure O_2 at 500°C for 60 min (heating rate of 5°C min^{-1}). After cooling down to room temperature, the sample was purged under Ar flow for 45 minutes. The reduction step was then carried out under 1 % H_2 in Ar flow up to 900°C, with a heating rate of 5°C min^{-1}. Since the TCD signal is sensitive to water, a trap (magnesium perchlorate) was added downstream of the reactor.

2.3. Catalytic tests

Tests were carried out in a quartz tubular micro-reactor under a flow representative of a Diesel exhaust gas (including CO_2, O_2, N_2, H_2O, NO_x) in which were added, alone or combined, various reductants: ammonia (NH_3), ethanol (EtOH) or acetaldehyde (CH_3CHO). All the catalytic test types are listed in Table 1. All tests were performed at a total flow rate of 333 mL

min^{-1}. For catalytic tests with single catalyst, 100 mg of powdered catalyst were diluted in 100 mg SiC, both sieved between 100 µm and 250 µm. The corresponding GHSV were of 130,000 h^{-1} toward Ag/Al and 230,000 h^{-1} toward WO_3/Ce-Zr catalysts (200 L h^{-1} g_{cata}^{-1}; 100 L h^{-1} g_{powder}^{-1}). Regarding the dual-bed configuration, 100 mg of WO_3/Ce-Zr catalyst were placed downstream 100 mg of Ag/Al catalyst. Consequently, the GHSV was of 180,000 h^{-1} (100 L h^{-1} g_{cata}^{-1}). The experimental setup has been previously described in [36,37]. The gas mixture was adjusted using Bronkhorst mass-flow controllers, except for ethanol, acetaldehyde and water which were vaporized into the reactor *via* a micro-nozzle (The Lee Company ($Ø_{nozzle}$= 50 µm)) placed into the quartz reactor in a heated zone at 200°C. The micro-nozzle was connected to a HPLC pump (Jasco, PU-2085) operating at a flow rate of 22 µL min^{-1}, (ΔP= 10 bar). Before injection, EtOH and CH_3CHO were diluted into water at a concentration of 8.02 10^{-1} mol L^{-1}, in order to achieve the desired amounts of reductant and water in the gas phase. Note that the theoretical residence time between the injection zone and the catalytic bed is 5.2 s.
The inlet and outlet gas compositions were monitored using a MKS 2030 Multigas infrared analyser, recording the concentrations of CH_3CH_2OH, CH_3CHO, CH_3OH, CH_2O, C_2H_4, CH_4, HCOOH, CO, CO_2, NO, NO_2, N_2O, NH_3, HNCO and H_2O.

Table 1. Gas mixtures for SCR catalytic tests (total flow rate: 333 mL min^{-1}).

Catalytic test	NO (ppm)	NO_2 (ppm)	NH_3 (ppm)	C_2-comp.[1] (ppm)	O_2 (%)	CO_2 (%)	H_2O (%)	N_2
Standard-NH_3-SCR	400	-	400	-	10	10	8	balance
Fast-NH_3-SCR	200	200	400	-	10	10	8	
EtOH-SCR	400	-	-	1200	10	10	8	
(EtOH+NH_3)-SCR	400	-	400	1200	10	10	8	
Fast-CH_3CHO-SCR	200	200	-	600	10	10	8	
Fast-(CH_3CHO+NH_3)-SCR	200	200	400	600	10	10	8	
CH_3CHO oxidation	-	-	-	600	10	10	8	

[1] C_2-compounds are C_2H_5OH (EtOH) or CH_3CHO

3. Results and discussion

3.1 Physical and chemical characterizations of Ag/Al and WO_3/Ce-Zr single catalysts

3.1.1. Ag/Al catalyst

The Ag/Al sample exhibited a specific surface area of 160 m^2 g^{-1}, which was very similar to the surface area of the host alumina support before the addition of 2 $_{wt}$% Ag (Table 2). The XRD analysis of this catalyst evidenced the γ-Al_2O_3 phase (ICDD PDF n° 00-050-0741(1)) and no peaks assigned to silver species such as Ag^0, Ag_2O or AgO were evidenced (Figure 1). TPR

profile of Ag/Al (not shown) exhibited a broad H_2 consumption peak centred at 260°C. The corresponding hydrogen consumption (Table 2). indicated that silver species were initially composed of 33 % of Ag^I species, in accordance with data reported by Musi *et al.* [35] for such samples. As previously reported in [29], TEM analysis showed that Ag/Al sample presented a homogeneous repartition of small silver particles, most of them ranging below 3 nm.

Table 2. Textural properties and hydrogen consumption from H_2-TPR experiments.

Catalyst	S_{BET} ($m^2.g^{-1}$)	porous volume ($cm^3.g^{-1}$)	mean pore diameter (Å)	TPR H_2 cons. (20-800°C range) ($\mu mol_{H2}.g^{-1}$)
Al	176	0.53	120	-
Ag/Al	160	0.49	128	119
Ce-Zr	73	0.32	175	795
WO_3/Ce-Zr	52	0.26	197	785

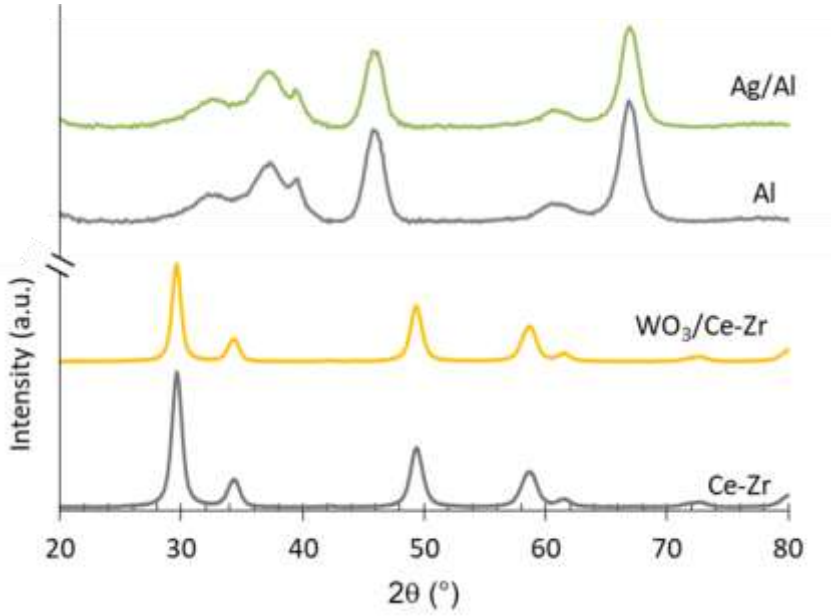

Figure 1: XRD patterns of the studied catalysts and corresponding host supports.

3.1.2. WO_3/Ce-Zr catalyst

The addition of 6 $_{wt}$% WO_3 to the ceria-zirconia support led to a significant decrease of the specific surface area, from 73 to 52 $m^2\ g^{-1}$. This decline was associated with a decrease in the porous volume from 0.32 to 0.26 $cm^3.g^{-1}$ and with an increase in the mean pore diameter from 175 to 197 Å (Table 2). The XRD analysis of WO_3/Ce-Zr revealed no modification of the XRD pattern of the support after WO_3 impregnation (Figure 1). No WO_3 XRD peaks were detected, suggesting a good dispersion of tungsten trioxide phase, in accordance with Xiaowei *et al.* [34] which reported that tungsten oxide can be highly dispersed on $Ce_{0.5}Zr_{0.5}O_2$ solid solution. The

H_2-TPR profile of WO_3/Ce-Zr (not shown) revealed a broad H_2 consumption peak between 350 and 750°C, with a maximum hydrogen consumption recorded at 660°C. The shoulder recorded in the low temperature range (350- 600°C) was attributed to the reduction of Ce^{4+} into Ce^{3+} from the first layers of the support, while the high temperature H_2 consumption was associated to the bulk reduction. No peak attributable to WO_3 was observed in the studied temperature range. A TPR experiment conducted over the $Ce_{40}Zr_{60}O_2$ support resulted in similar profile, with an identical H_2 consumption (Table 2). Only a shift of approximately 50°C to lower temperatures was observed. It suggests interactions between deposited WO_3 and the support which slowed down the support reducibility, in accordance with a previous study [13]. These results together with XRD patterns allow to assume that WO_3 covered the Ce-Zr support without causing any structural change for the support.

3.2. Catalytic activity of WO_3/Ce-Zr in NO_x SCR by NH_3 and/or EtOH.

In order to have a better understanding of the WO_3/Ce-Zr behaviour in the Ag/Al + WO_3/Ce-Zr dual-bed system, the catalytic activity of single WO_3/Ce-Zr was examined with various gas mixtures detailed in section 2.3.

3.2.1. Standard and fast-NH_3-SCR conditions

Single WO_3/Ce-Zr catalyst was firstly evaluated in NH_3-SCR with two different NO_2/NO_x inlet ratios corresponding to the standard-SCR condition (NO_2/NO_x= 0) and to the fast-SCR condition (NO_2/NO_x= 0.5). Obtained NO_x and NH_3 conversions are reported in Figures 2a and 2b, respectively. In standard-SCR condition (Figure 2a), the NO_x conversion was ranked between 15 % and 90 % in the 175 - 300°C temperature range. In this temperature range, the NH_3 conversion followed the same trend, in accordance with the standard-SCR stoichiometry (reaction (1)), corresponding to an ammonia to NO_x ratio (ANR) of 1. A decrease in the NO_x conversion was then observed for temperatures higher than 450°C, while ammonia was totally converted. The NO_x reduction then competed with the ammonia oxidation, which can lead to either N_2 or NO_x as described by reactions (3) and (4) [6]:

$$4\ NH_3 + 3\ O_2 \rightarrow 2\ N_2 + 6\ H_2O \qquad (3)$$

$$4\ NH_3 + 5\ O_2 \rightarrow 4\ NO + 6\ H_2O \qquad (4)$$

Note that N_2O could be a by-product of both the NH_3 oxidation and the NO_x reduction. However, these pathways were very limited since N_2O was detected only in small amounts in both standard and fast-SCR condition (less than 10 ppm over the full studied temperature range).

As expected, the NO_x conversion was significantly improved in fast-SCR condition (Figure 2b). Compared to the standard-SCR condition, the NO_x conversion was increased by around 30 and 50 % at 175°C and 200°C, respectively. The 90 % NO_x conversion was reached from 200°C in fast-SCR condition while a temperature higher than 250°C was needed in standard-SCR condition. The ammonia conversion still followed the NO_x conversion until 400°C, according to the 1:1 stoichiometric ratio resulting from the fast-SCR reaction (2). Again, a decrease in the NO_x conversion was observed for temperature higher than 450°C due to the competition with the ammonia oxidation.

Finally, as expected, a clear improvement in the NO_x conversion was obtained when NO and NO_2 were fed together. Mechanistic studies highlighted that the concomitance of NO and NO_2

favours the formation of surface HNO_x species, which are very reactive towards ammonia [38]. When only NO is introduced in the gas mixture, the limiting step corresponds to the oxidation of NO to NO_2 [39] to further obtain the formation of HNO_x species. To characterize the NO oxidation ability of the WO_3/Ce-Zr sample, a supplementary test was performed without ammonia in the feed stream. Results (not shown) showed that this catalyst was unable to significantly oxidize NO in NO_2 below 350°C, which explains the lack of activity in standard-SCR condition at low temperature.

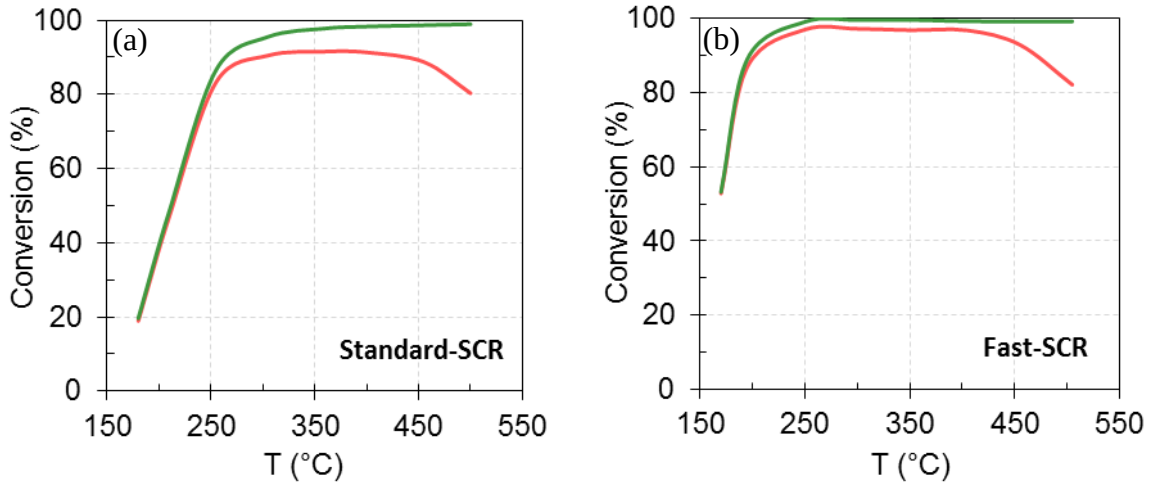

Figure 2. NO_x (—) and NH_3 (—) conversions in NH_3-SCR over WO_3/Ce-Zr catalyst for standard-NH_3-SCR condition (**a**) and fast-NH_3-SCR condition (**b**). Reaction mixtures are depicted in Table 1.

3.2.2. EtOH and (EtOH+NH_3)-SCR conditions

In the dual-bed (Ag/Al+WO_3/Ce-Zr) catalytic system, the silver-based catalyst is dedicated to the EtOH-SCR purpose (see section 3.3). However, mixtures including ethanol (and its by-products) may reach the WO_3/Ce-Zr catalyst placed downstream. Consequently, the single WO_3/Ce-Zr catalyst was also evaluated in EtOH-SCR and (EtOH+NH_3)-SCR conditions with only NO as injected NO_x, as reported in Table 1.

EtOH-SCR tests were performed by injecting 1200 ppm of EtOH in the feed-stream (without ammonia). NO_x and EtOH conversion profiles recorded over WO_3/Ce-Zr are presented in Figure 3a, while outlet concentrations of NO_2 and C-compounds are presented in Figure 3b. The catalyst allowed the ethanol conversion from the starting temperature (175°C) and EtOH was completely converted at 320°C (Figure 3a). However, the NO_x conversion was then very limited, with a maximum of 7 % around 300°C. For temperatures higher than 350°C, few amounts of NO_2 were emitted, with a maximum of 30 ppm observed at 500°C (Figure 3b, blue line). In this temperature range, NO oxidation into NO_2 was probably resulting from the reaction between NO and ethanol in the gas phase, as already mentioned in the literature [22].

The ethanol conversion over WO_3/Ce-Zr was firstly characterized by the formation of small amounts of acetaldehyde, with a maximum of 160 ppm recorded at 250°C (Figure 3b). The ethanol reactivity was also characterized by the emission of high concentrations of ethylene and CO from 300°C. In this temperature range, the catalyst thus promoted the dehydration reaction

rather than the dehydrogenation reaction of ethanol. Moreover, ammonia was not detected as a reaction product. As discussed in the introduction part, ammonia emission is usually observed over Ag/Al_2O_3 catalysts in EtOH-SCR condition. Its formation is due to the decomposition of nitromethane, an intermediate species involved in the N_2 formation route. Ammonia absence over WO_3/Ce-Zr indicates that nitromethane formation was then limited or did not occur. It results that WO_3/Ce-Zr catalyst is not efficient to reduce NO_x by ethanol, probably because of the acidity procured by WO_3, which generally promotes alcohols dehydration [40,41].

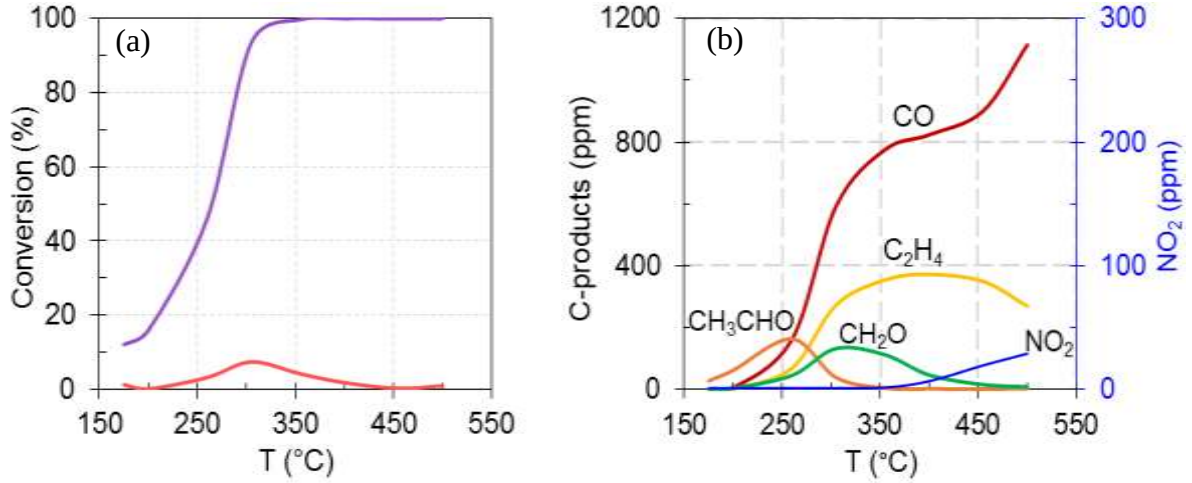

Figure 3. EtOH-SCR over WO_3/Ce-Zr catalyst: NO_x (—) and EtOH (—) conversions (**a**) and CH_3CHO (—), CO (—), CH_2O (—), C_2H_4 (—) and NO_2 (—) distributions (**b**). Reaction mixture is depicted in Table 1.

The single WO_3/Ce-Zr catalyst was also evaluated in ($EtOH+NH_3$)-SCR condition (Figure 4). To the opposite of EtOH-SCR (Figure 3), the NO_x conversion was significant in ($EtOH+NH_3$)-SCR condition, from 13 to 70 % in the 175 – 450°C temperature range (Figure 4a). Above 450°C, the conversion dropped slightly. This reactivity was correlated with the conversion of ammonia. From 175 to 250°C, the NH_3 conversion was close to the NO_x conversion, indicating that the standard-SCR reaction was achieved. From 250°C, the NH_3 conversion became higher than the NO_x conversion, reaching 93 % at 350°C. The NO_x conversion loss at T > 450°C was thus correlated to the probable oxidation of a part of the added ammonia, according to reaction (3) and (4).

However, in comparison to the standard-NH_3-SCR test reported in Figure 2a, the NO_x conversion in ($EtOH+NH_3$)-SCR was significantly lower. For instance, the NO_x conversion at 250°C was more than two times lower in presence of ethanol, at around 40 % compared to 85 % in NH_3-SCR. Thus, the presence of ethanol did not allow NO_x conversion but also inhibited the NH_3-SCR over WO_3/Ce-Zr. This statement was confirmed by the comparison of the EtOH conversion profiles. Compared to EtOH-SCR experiments (Figure 3a), NH_3 co-injection induced a slight decrease in the ethanol conversion, especially in the 250-300°C temperature range. As a result, lower amounts of acetaldehyde were also observed (Figure 4b). Similarly, NH_3 conversion also decreased in presence of ethanol. A competitive adsorption between the two reductants is thus presumed, probably occurring on the acid sites. As for EtOH-SCR

condition, NO_2 emissions were recorded in (EtOH+NH_3)-SCR, but in a lower extent. A maximum of 15 ppm was observed at 500°C, suggesting a consumption of emitted NO_2 with NH_3.

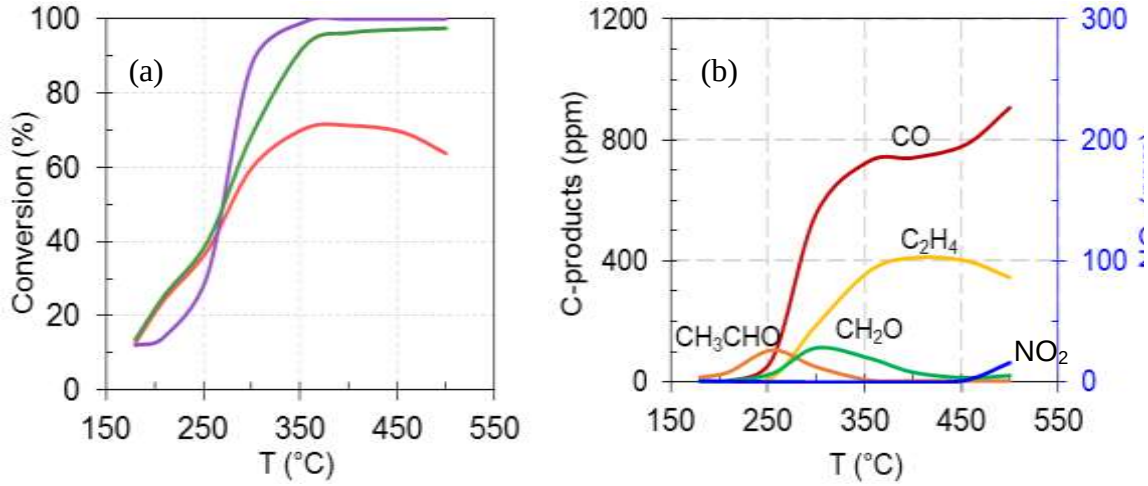

Figure 4. (EtOH+NH_3)-SCR over WO_3/Ce-Zr catalyst: NO_x (—), NH_3 (—) and EtOH (—) conversions (**a**) and CH_3CHO (—), CO (—), CH_2O (—), C_2H_4 (—) and NO_2 (—) distributions (**b**). Reaction mixtures are depicted in Table 1.

To conclude, the WO_3/Ce-Zr catalyst is quite inactive for reducing NO_x with ethanol. In addition, the comparison of the $DeNO_x$ efficiency over WO_3/Ce-Zr catalyst in (EtOH+NH_3)-SCR (Figure 4a) and NH_3-SCR (Figure 2a) with only NO as NO_x injected revealed a lower NO_x conversion when ethanol was co-fed with ammonia. It suggests a competitive adsorption of ethanol or these by-products with NH_3. This assumption is also consistent with the lower ethanol conversion reported for (EtOH+NH_3)-SCR compared to EtOH-SCR. In the context of the dual-bed catalytic system, there is therefore a risk that residual ethanol and carbonaceous by-products (after passing through the first Ag/Al catalytic bed) partially inhibit the activity of the second bed (WO_3/Ce-Zr).

3.3. Catalytic behaviours of Ag/Al and Ag/Al + WO_3/Ce-Zr dual-bed

In order to highlight the reactivity of the WO_3/Ce-Zr in the dual-bed configuration (composed of 100 mg of Ag/Al as EtOH-SCR catalyst placed upstream 100 mg of WO_3/Ce-Zr as NH_3-SCR catalyst), results were compared with those obtained over single Ag/Al catalyst (100 mg diluted in 100 mg of SiC). The $DeNO_x$ chemistry of Ag/Al sample in EtOH-SCR and (EtOH+NH_3)-SCR was already discussed in a previous work [29]. As presented in the introduction section, one interesting point is the significant NO_2 emission recorded at low temperature (175 – 300°C) concomitantly with ethanol oxidation into CH_3CHO.

3.3.1. EtOH-SCR condition

Ag/Al and the dual-bed configuration were firstly evaluated in EtOH-SCR (1200 ppm EtOH, 400 ppm NO, 10 % O_2, 10 % CO_2, 8 % H_2O, N_2).

3.3.1.1. Evolution of C-compounds (ethanol and acetaldehyde)

Figure 5 reports the ethanol conversions and the acetaldehyde emission obtained in EtOH-SCR for both catalytic configuration. Compared with single Ag/Al catalyst, the ethanol conversion was enhanced over the dual-bed system, by 10 to 20 % in the 175 - 350°C temperature range. This improvement is explained by the ability of the WO_3/Ce-Zr catalyst to activate the oxidation of ethanol from 175°C, as previously illustrated in Figure 3a. Interestingly, the acetaldehyde concentration was also impacted by the addition of WO_3/Ce-Zr. A significant decrease was observed from 200°C. At 250°C, a maximum of 420 ppm was reached over Ag/Al, while the concentration was almost three times lower (150 ppm) over the dual-bed system. Instead, according to Figure 3b, an additional release of CH_3CHO was rather expected by the addition of the second bed. Therefore, this consumption, recorded over a wide temperature range, suggests a specific reactivity of acetaldehyde over WO_3/Ce-Zr sample. This point is discussed thereafter in section 3.3.2.

Note that the CO emission from the dual-bed configuration (not shown) was close to that observed with Ag/Al alone and significantly lower than values recorded with WO_3/Ce-Zr sample. For instance, at 350°C (temperature for which the ethanol conversion reached 100 % for the three studied catalytic beds), the CO emissions reached 245, 765 and 325 ppm over the Ag/Al, WO_3/Ce-Zr and Ag/Al+WO_3/Ce-Zr catalytic systems, respectively. Then, the addition of WO_3/CeZr downstream Ag/Al led only to a small increase of the CO emissions, indicating that other by-products from ethanol decomposition, typically CH_3CHO, were partially converted into CO over WO_3/CeZr (see also section 3.3.3).

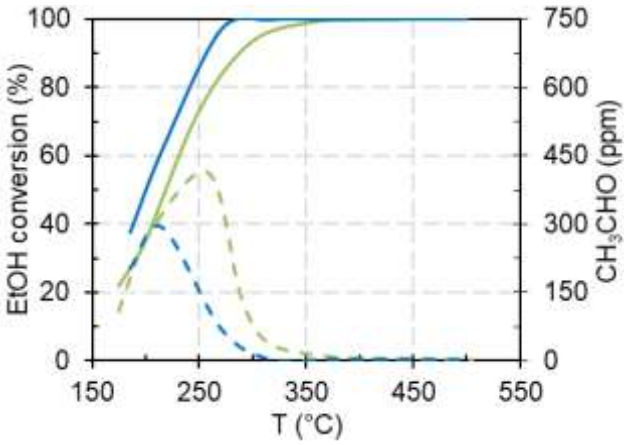

Figure 5. EtOH-SCR over Ag/Al (—) and (Ag/Al+WO_3/Ce-Zr) dual-bed system (—): EtOH conversions (full line) and CH_3CHO emissions (dotted line). Reaction mixtures are depicted in Table 1.

3.3.1.2. Evolution of N-compounds

The NO_x conversion and NO_2 concentration profiles recorded during the EtOH-SCR experiments are depicted in Figure 6 depending on the nature of the catalyst bed,. As expected, the addition of WO_3/Ce-Zr downstream Ag/Al catalyst led to an enhancement in the $DeNO_x$ efficiency in the 230 - 400°C temperature range.

This improvement can be related to the capacity of the Ag/Al catalyst to generate NH_3 *in situ* as reported by Flura *et al.* [22], which can be used by the NH_3-SCR catalyst. Indeed the NH_3 emission was significantly decreased after the addition of the WO_3/Ce-Zr. For instance, 19 ppm NH_3 were converted on WO_3/Ce-Zr at 300°C, close to the supplementary NO_x conversion (16 ppm). At higher temperature, when the NO_x conversion already reached 100 % over Ag/Al, the WO_3/Ce-Zr catalyst also acted as an ammonia slip catalyst, limiting the ammonia emissions: at 400°C, 98 ppm NH_3 were converted while the NO_x conversion remained total. Unfortunately, for temperature higher than 450°C, the ammonia oxidation appeared leading to NO_x formation, since a decrease in the NO_x conversion was then observed (Figure 6).

Besides, Figure 6 shows that the outlet concentration of NO_2 was also strongly affected by the addition of the second catalytic bed. Indeed, NO_2 was fully consumed from 175 to 400°C whereas amounts higher than 220 ppm were emitted from Ag/Al catalyst between 200 and 250°C. Thanks to ammonia formation on the first bed, NO_2 could be potentially reduced, according to the fast SCR reaction (reaction (2)). This result would be in accordance with the strong activity of the WO_3/Ce-Zr catalyst in fast condition (section 3.2.1). However, the NO_2 consumption on WO_3/Ce-Zr was too important to be only explained by the fast SCR reaction, with respect to the gain of NO_x conversion observed by adding the NH_3-SCR catalyst. Then, a realistic assumption is that NO_2 was also reduced into NO over WO_3/Ce-Zr catalyst. Moreover, the NO_2 consumption was also concomitant with the improvement in the acetaldehyde consumption (Figure 5), suggesting that both species could be involved in an additional reaction. This assumption is examined in section 3.3.3.

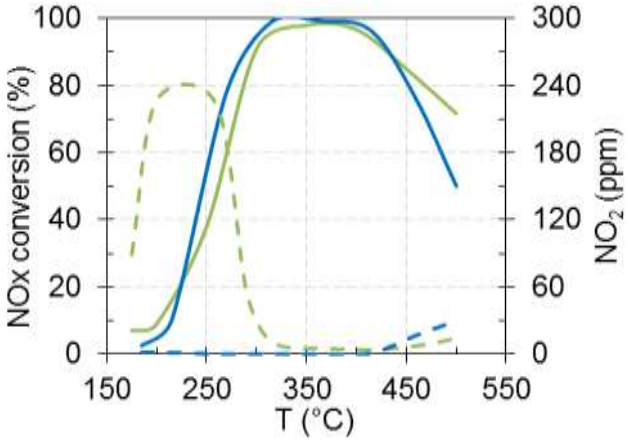

Figure 6. EtOH-SCR over Ag/Al (—) and (Ag/Al+WO_3/Ce-Zr) dual-bed system (—): NO_x conversions (full line) and NO_2 emissions (dotted line). Reaction mixtures are depicted in Table 1.

3.3.2. (EtOH+NH_3)-SCR condition

Both Ag/Al and Ag/Al+WO_3/Ce-Zr catalytic systems were also compared in (EtOH+NH_3)-SCR (1200 ppm EtOH, 400 ppm NH_3, 400 ppm NO, 10% O_2, 10% CO_2, 8% H_2O).

3.3.2.1. Evolution of C-compounds (ethanol and acetaldehyde)

Figure 7 shows the influence of the addition of the WO_3/Ce-Zr catalyst to Ag/Al toward both ethanol conversion and acetaldehyde emission measured in (EtOH+NH_3)-SCR condition.

When NH_3 was added to the inlet mixture, similar ethanol conversion profiles were obtained whatever the catalytic bed configuration. Compared to single Ag/Al, the dual-bed led to a slight increase in the alcohol conversion, as already reported in EtOH-SCR condition. Again, the acetaldehyde emission was decreased by addition of the WO_3/Ce-Zr catalyst. Nevertheless, over the dual-bed system, co-injection of (EtOH+NH_3) led to a lower acetaldehyde outlet concentration than that observed in EtOH-SCR condition, suggesting a competitive reactivity of acetaldehyde with co-fed ammonia. However, whatever the considered catalytic system, the addition of NH_3 in the inlet mixture has no significant impact on CO emissions.

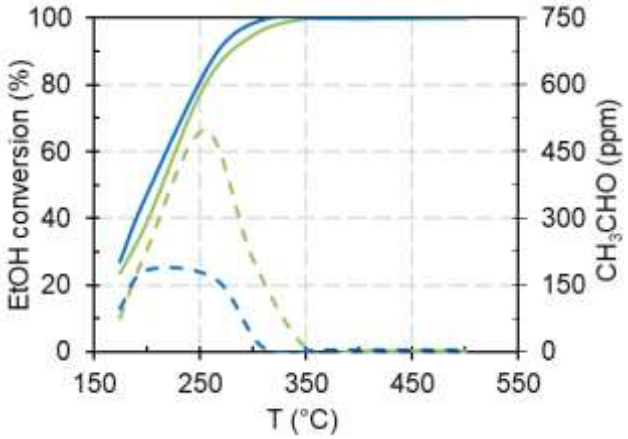

Figure 7. (EtOH+NH_3)-SCR over Ag/Al (—) and (Ag/Al+WO_3/Ce-Zr) dual-bed system (—): EtOH conversions (full line) and CH_3CHO emissions (dotted line). Reaction mixtures are depicted in Table 1.

3.3.2.2. Evolution of N-compounds

Figure 8 reports the evolution of the N-compounds, expressed as the NO_x conversion and the NO_2 emission profiles for both catalytic systems. As expected, the addition of ammonia to the feed-stream led to a remarkable enhancement of the $DeNO_x$ activity compared to the NO_x conversions obtained over the single Ag/Al catalyst, especially at low temperature (T < 300°C). The NO_x conversion was then ranked between 45 and 90 % in the 175 - 250°C temperature range, while only NO was initially injected. Interestingly, the $DeNO_x$ efficiency obtained in (EtOH+NH_3)-SCR condition over the dual-bed system became close to the activity observed in the most favourable fast-SCR stoichiometry recorded with single WO_3/Ce-Zr sample (Figure 2a).

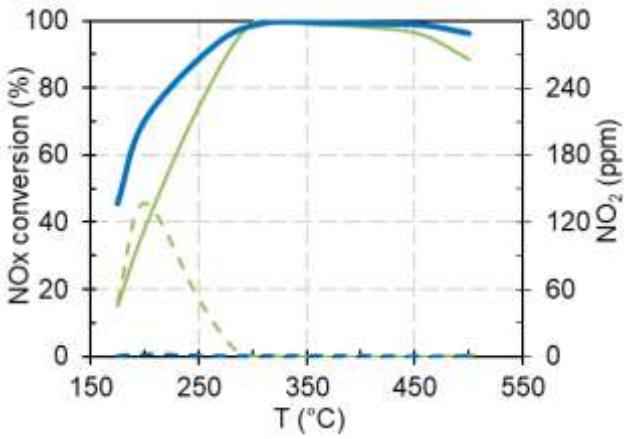

Figure 8. (EtOH+NH_3)-SCR over Ag/Al (—) and (Ag/Al+WO_3/Ce-Zr) dual-bed system (—): NO_x conversions (full line) and NO_2 emissions (dotted line). Reaction mixtures are depicted in Table 1.

As previously observed in EtOH-SCR condition, NO_2 emitted from Ag/Al was fully converted in the dual-bed configuration. Table 3 reports, for each studied temperature, the amounts of NH_3, NO_2 and NO_x converted by the second WO_3/Ce-Zr bed by subtraction between the remaining amounts measured after single Ag/Al bed and the dual-bed (remind that 400 ppm NH_3 were then added in the feed stream). Table 3 clearly evidenced that the addition of the NH_3-SCR catalyst led to a significant supplementary ammonia consumption. For a temperature higher than 300°C, for which the gain in NO_x conversion is negligible, WO_3/Ce-Zr catalyst acted as an ammonia slip catalyst, limiting the ammonia emissions. In the 175 – 250°C temperature range, the improvement in the ammonia conversion was associated with an improvement in the NO_x conversion. However, data clearly evidenced that the involved NO_x and NH_3 quantities did not correspond to the stoichiometry of the fast or standard SCR reactions described in reactions (1) and (2).

Table 3. NH_3 outlet emissions recorded in (EtOH+NH_3)-SCR over Ag/Al catalyst and the dual-bed catalytic system (Ag/Al+WO_3/Ce-Zr); NH_3, NO_x and NO_2 consumptions resulting from the addition of WO_3/Ce-Zr catalyst downstream Ag/Al (for instance, ΔNH_3= NH_3(Ag/Al)-NH_3(dual-bed)).

Temperature (°C)	NH_3 outlet (ppm)		ΔNH_3 (ppm)	ΔNO_x (ppm)	ΔNO_2 (ppm)
	Ag/Al	Dual-bed			
175	363	223	140	49	127
200	300	115	185	137	124
250	195	125	70	52	36
300	304	229	75	1	1
350	351	265	86	0	3
400	339	192	147	0	6
450	306	70	236	0	19
500	256	18	238	2	47

In order to obtain a better understanding of the reactions involved, the amounts of NO_2 and NH_3 consumed by the addition of WO_3/Ce-Zr were used to predict the NO_x conversion. The theoretical NO_x conversion was calculated assuming two different hypothesis: (i) the supplementary NO_2 consumption was only used to carry out the fast SCR reaction; the consumption of NO_2 was therefore doubled to obtain the theoretical NO_x conversion, to take into account that NO was also equally consumed by the fast SCR reaction; (ii) the supplementary consumed NH_3 was only used to reduce NO_x, with a NH_3:NO_x ratio of 1:1. These estimations of NO_x conversion were then added to the experimental values obtained in (EtOH+NH_3)-SCR over the single Ag/Al catalyst to obtain a theoretical NO_x conversion over the dual-bed system. Results from these calculations are presented in Figure 9 as a function of temperature, and compared to the experimental NO_x conversion obtained with the dual-bed configuration. When the NO_x conversion was estimated from the quantity of consumed NH_3 (green bares), the comparison to the experimental value (blue bares) shows rather close NO_x conversion in the 175-250°C temperature range, which suggests that the supplementary NO_x conversion was mainly governed by the standard or, more probably, the fast-SCR reaction (both respecting a NH_3:NO_x ratio of 1). However, at T ≥ 300°C, the calculated NO_x conversion was then higher than 100%, reaching up to 155% at 450°C. This result induces an overconsumption of ammonia that could be attributed to its oxidation (SCO) into N_2, according to reaction (3). This reaction is usually undesired because it leads to an overconsumption of the reductant. Moreover, depending on the catalyst and the temperature, ammonia SCO can lead to NO_x formation, according to reaction (4). The efficiency of the WO_3/Ce-Zr catalysts toward SCO reaction was already described in [13]. The ammonia conversion started near 250°C and reached approximately 80 % at 500°C. N_2O was not detected and traces of NO_x (in fact NO) were only detected at 500°C. The corresponding NO selectivity was then lower than 5 %.

When the NO_x conversion was estimated from the amount of NO_2 consumed (red-grey bares) by considering a fast-SCR stoichiometry, the only calculation closed to the experimental value was obtained at 175°C and thus could characterize a fast-SCR type reaction. The values calculated at 200°C and 250°C were significantly higher than the experimental values, even exceeding a theoretical conversion of 100 %. These results highlight that NO_2 was not only consumed for the NO_x reduction, but NO_2 was partially reduced into NO. Indeed, NO_2 reduction is possibly related to the oxidation of acetaldehyde, its consumption (Figure 7) being also significant in the same temperature range. This hypothesis is developed in the following section.

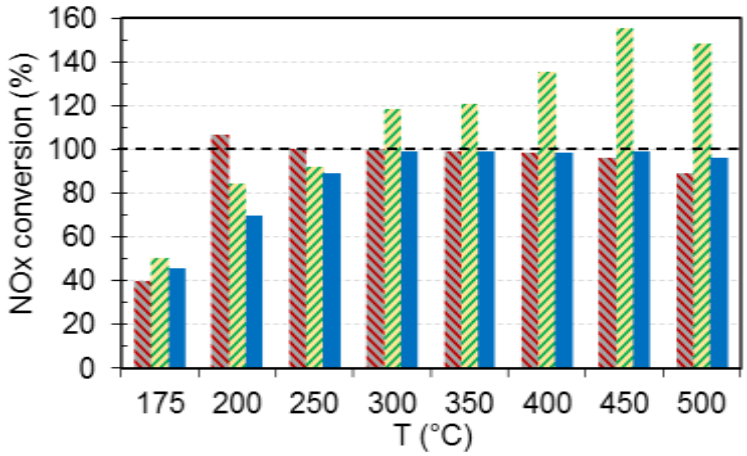

Figure 9. Additional NO_x conversion expected from N-balance during ($EtOH+NH_3$)-SCR test over the dual-bed configuration (Ag/Al+WO_3/Ce-Zr). (▨): additional NO_x conversion estimated from NO_2 consumption by WO_3/Ce-Zr (according to the fast SCR stoichiometry); (▨): additional NO_x conversion estimated from NH_3 consumption over WO_3/Ce-Zr; (■): experimental NO_x conversion measured in ($EtOH+NH_3$)-SCR over the dual-bed system.

3.3.3. Acetaldehyde - NO_2 reactivity

Results obtained in dual-bed configuration in both EtOH-SCR and ($EtOH+NH_3$)-SCR conditions (sections 3.3.1 and 3.3.2, respectively) showed that the NO_2 consumption over WO_3/Ce-Zr was not only involved in the NO_x reduction respecting the fast-SCR reaction, and was also concomitant with the increase in the acetaldehyde consumption. Focussing on the ($EtOH+NH_3$)-SCR condition and according to Table 3, 137 ppm of NO_2 were consumed at 200°C after addition of WO_3/Ce-Zr to Ag/Al. Assuming that the NO_x conversion gain was exclusively associated with the fast-SCR reaction, it would correspond to the conversion of 64 ppm NO_2 + 64 ppm NO. Around 70 ppm of remaining NO_2 were then converted into NO. This value being in the same order than the acetaldehyde consumption after the addition of the second bed, the reaction (5) was then hypothetically proposed:

$$CH_3CHO + NO_2 + 2\ O_2 \rightarrow NO + 2\ CO_2 + 2\ H_2O \quad (5)$$

NO_2 is well known to be a stronger oxidizer than O_2. For instance, NO_2 is commonly used for particulate matter removal in vehicles [4,42], it favours the continuous regeneration of the diesel particulate filter (DPF). Consequently, the improvement in the acetaldehyde oxidation in presence of NO_2 is actually conceivable.

Even if reaction (5) probably occurred at 200°C over WO_3/Ce-Zr, it did not reflect the NO_2-CH_3CHO reactivity in the whole studied temperature range. Indeed, the ratio between consumed CH_3CHO and NO_2 over WO_3/Ce-Zr was temperature dependant. Furthermore, this reaction supposes a complete CH_3CHO oxidation into CO_2. The fact that other compounds such as remaining ethanol but also CO, C_2H_4 and CH_2O produced over the first bed could also reacted on the second bed impedes in determining if CH_3CHO oxidation by NO_2 was completed or not. In addition, over the dual-bed system, supplementary formaldehyde emissions of 20 and 63 ppm were observed at 200°C and 250°C, respectively, compared to single Ag/Al. Then, the complex mixture reaching the WO_3/Ce-Zr catalyst led to numerous secondary reactions.

In order to investigate in greater depth the reaction between acetaldehyde and NO_2 over WO_3/Ce-Zr catalyst, supplementary catalytic tests were performed over single WO_3/Ce-Zr using acetaldehyde instead of ethanol as introduced reductant. The CH_3CHO concentration for these tests was fixed at 600 ppm to be consistent with the acetaldehyde concentration recorded from Ag/Al sample. Figure 10 reports the CH_3CHO conversion evaluated under different conditions reported in Table 1: (i) oxidation test with O_2 (600 ppm CH_3CHO, without NO_x), (ii) fast-CH_3CHO-SCR (600 ppm CH_3CHO, 200 ppm NO, 200 ppm NO_2) and (iii) fast-(CH_3CHO+NH_3)-SCR (400 ppm NH_3 supplementary added). Note that the conversions are only reported at low temperatures (between 175 and 300°C), because total CH_3CHO conversion was recorded at a higher temperature over Ag/Al.

It clearly appears that WO_3/Ce-Zr is active in CH_3CHO oxidation with O_2, with 90 % conversion at 300°C (blue bare). Interestingly, for temperature ranked between 175 and 250°C, higher acetaldehyde conversions were denoted in the fast-CH_3CHO-SCR condition (grey bare). Consequently, these results are in accordance with the hypothesis of a NO_x-CH_3CHO reactivity. When NH_3 was co-fed with CH_3CHO (green bare), the conversion was slightly lower. Thus, a competitive adsorption between CH_3CHO and NH_3 was highlighted, such as already observed with ethanol.

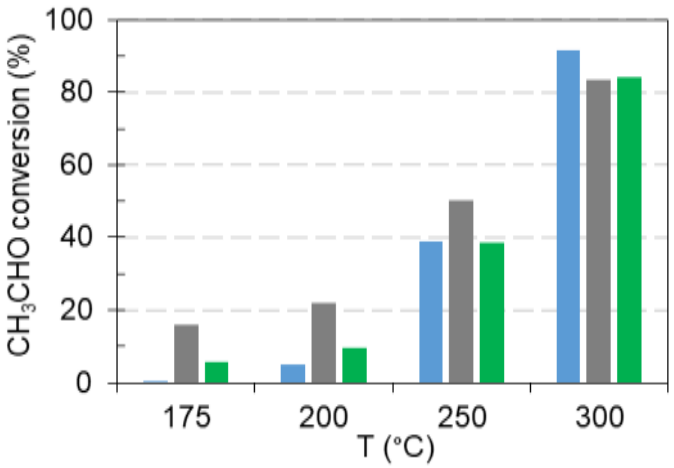

Figure 10. Comparison of the CH_3CHO conversion *vs* the temperature, recorded over WO_3/Ce-Zr for three different tests: CH_3CHO oxidation with O_2 (■), fast-CH_3CHO-SCR (■) and fast-(CH_3CHO+NH_3)-SCR (■).

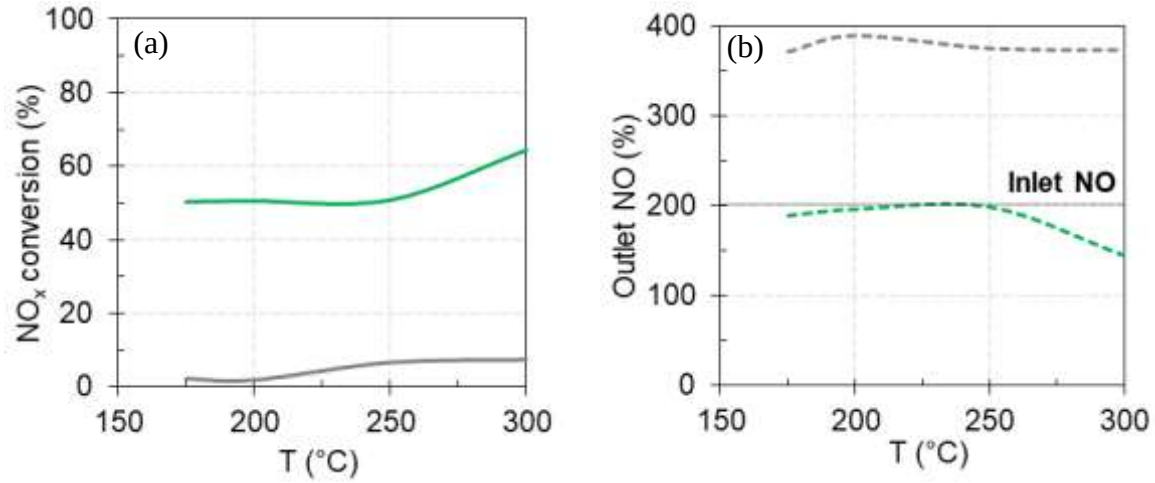

Figure 11. Comparison of the NO_x conversion ((a), full line) and the NO outlet emission ((**b**), dotted line) *vs* the temperature, recorded over single WO_3/Ce-Zr catalyst in fast-CH_3CHO-SCR (—) and in fast-(CH_3CHO+NH_3)-SCR (—). Reaction mixtures are depicted in Table 1.

The NO_x conversion and the NO outlet emission recorded over single WO_3/Ce-Zr catalyst in fast-CH_3CHO-SCR and fast-(CH_3CHO+NH_3)-SCR conditions are reported in Figure 11a and Figure 11b, respectively. In fast-CH_3CHO-SCR condition, the $DeNO_x$ efficiency was limited to 7 % between 250°C and 300°C (full grey line). Interestingly, this result could explain a part of the $DeNO_x$ enhancement recorded in the same temperature range in EtOH-SCR condition over the dual-bed system (see section 3.3.1). In parallel, from 175°C, a major part of the introduced NO_2 was reduced into NO (Figure 11b) since NO emission was superior to 370 ppm over the whole studied temperature range, while only 200 ppm were introduced. This result confirms once again the reaction between acetaldehyde and NO_2, as proposed in reaction (5).
However, the CH_3CHO-NO_2 stoichiometry appeared varying with temperature. For instance, at 175°C in the fast-CH_3CHO-SCR condition, 175 ppm of NO_2 were consumed for the oxidation of 100 ppm of CH_3CHO (16 % of CH_3CHO conversion, grey bare Figure 10), which results in a NO_2/CH_3CHO ratio of 1.75. Besides, this ratio seems to be the most precise we can determine because no consumption of CH_3CHO by O_2 was denoted at this temperature in oxidation reaction (blue bare, Figure 10). Only the CH_3CHO conversion linked with NO_2 was involved. It should also be noted that the stoichiometry proposed in reaction (5) assumes a total oxidation of acetaldehyde by NO_2, which is not entirely correct. Indeed, other carbon by-products than CO_2 were detected, mainly HCOOH, CO and CH_2O, showing an incomplete oxidation of CH_3CHO. Taking into account (i) all these detected carbon by-products and (ii) the observed NO_2/CH_3CHO consumption ratio, the experimental stoichiometry calculated at 175°C would correspond to reaction (6):

$$35\ NO_2 + 20\ CH_3CHO + 10\ O_2 \rightarrow 35\ NO + 12\ CH_2O + 13\ H_2O + 6\ CO + 15\ HCOOH + 7\ CO_2 \quad (6)$$

Clearly, this equation includes several reactions occurring on the catalyst surface, going from the partial CH_3CHO oxidation to its complete oxidation into CO_2.
Figure 11b also revealed that the NO_x conversion was enhanced in presence of NH_3 (green curve), assigned to the activity of WO_3/Ce-Zr sample in NH_3-SCR (Figure 2). For instance, a

NO_x conversion of 50 % was achieved at 175°C, close to the value obtained with only ammonia as reducer (about 55 %). In this case, the over-emission of NO was not observed, with a preferentially NO_2 reduction into N_2. It induced that the NO_x reduction by NH_3 appeared more favoured than the acetaldehyde oxidation by NO_2. However, the NO_x conversion reached only 50 – 60 % between 200°C and 300°C, indicating an inhibitory effect from acetaldehyde on the fast-NH_3-SCR reaction. Finally, these specific tests confirmed both the reactivity of CH_3CHO with NO_2 and the competitive adsorption of CH_3CHO with ammonia over WO_3/Ce-Zr. To summarize, an overview of the various reaction pathways identified in the (EtOH+NH_3)-SCR process over the (Ag/Al + WO_3/Ce-Zr) dual-bed system is presented in Figure 12. Pathways over Ag/Al catalyst originate from our previous work [29]. Despite the beneficial collaborative effect of ethanol and NH_3 on the NO_x conversion over silver supported catalyst, mainly attributed to the so-called "H_2 assisted" NH_3 –SCR, some NO, NO_2 and NH_3 remained at low temperature, as well as few hundreds ppm of acetaldehyde from ethanol decomposition. The reactivity of these remaining compounds results in three main reaction pathways on WO_3/Ce-Zr catalyst. Firstly, as expected, the addition of this NH_3-SCR catalyst allowed the improvement of the low temperature deNO_x efficiency *via* the favorable fast-SCR reaction, but an inhibiting effect of traces of acetaldehyde was also highlighted. Secondly, a part of NO_2 emitted from Ag/Al was not used for the fast-SCR reaction but reacted with CH_3CHO to form NO, with also formation of traces of HCOOH, CO and CH_2O. Thirdly, note that for temperature higher than 250-300°C, NH_3 is also emitted from Ag/Al [22,29] while the NO_x conversion was total. The added WO_3/Ce-Zr catalyst then acted as an ammonia slip catalyst (ASC) allowing the selective ammonia oxidation into N_2.

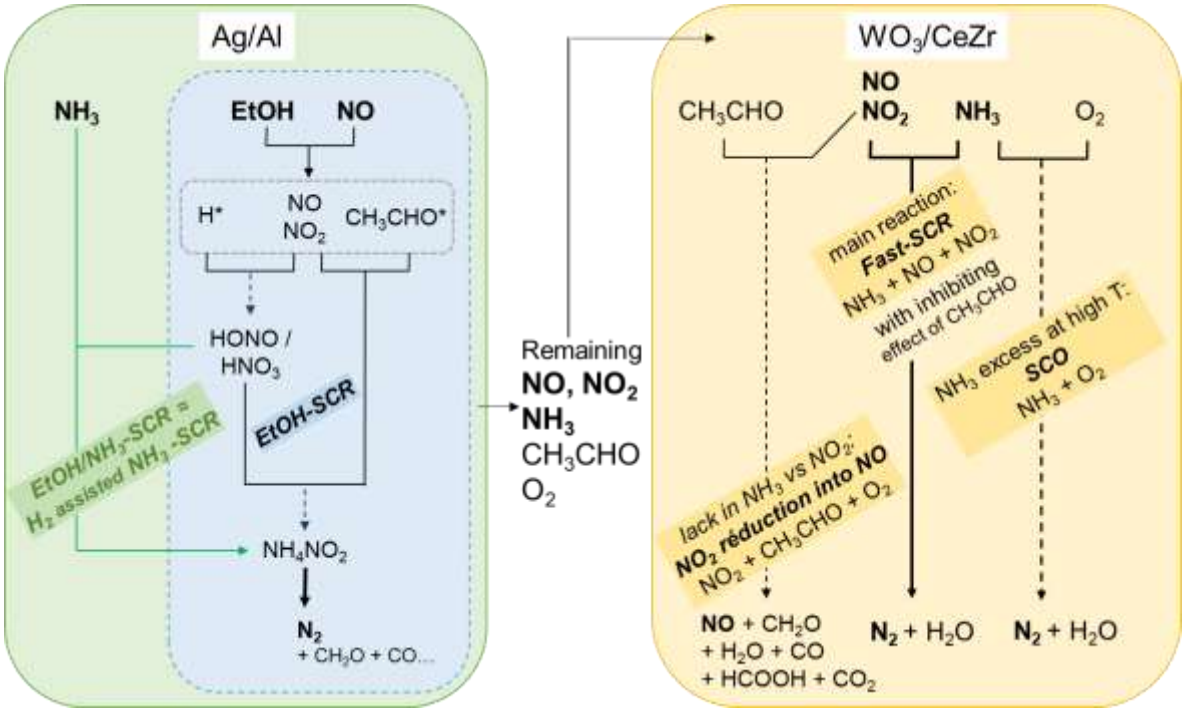

Figure 12. Schematic view of the various reaction pathways identified in the (EtOH+NH_3)-SCR process over the (Ag/Al + WO_3/Ce-Zr) dual-bed system.

4. Conclusions

The (EtOH+NH_3)-SCR process is an efficient way to reach stricter NO_x emission regulations without dependency to the NO_2/NO_x ratio provided by the DOC upstream. This high $DeNO_x$ performance was achieved by a dual-bed configuration composed of an EtOH-SCR catalyst upstream a NH_3-SCR catalyst (Ag/Al_2O_3+WO_3/Ce_x-Zr_yO_2). The emitted NO_2 by the EtOH-SCR sample allowed the favorable fast-SCR reaction on the downstream NH_3-SCR catalyst. Unfortunately, the NH_3-SCR reactivity over WO_3/Ce_x-Zr_yO_2 was not optimal because of (i) a competitive adsorption between ammonia and ethanol/acetaldehyde and (ii) an undesired NO_2 reactivity with CH_3CHO to form NO. In addition, CH_3CHO-SCR experiments over single WO_3/Ce_x-Zr_yO_2 also pointed out the formation of several by-products from the partial oxidation of CH_3CHO such as HCOOH, CO, CH_2O. Then, the beneficial effect of WO_3/Ce_x-Zr_yO_2 as the second bed appeared not optimal, but this (Ag/Al_2O_3+WO_3/Ce_x-Zr_yO_2) combination remained significantly more attractive than (Ag/Al_2O_3+Cu-FER) previously studied in (EtOH+NH_3)-SCR.

Acknowledgement: This research was funded by the Regional Council of Nouvelle Aquitaine, the French Ministry of Research and the European Regional Development Fund (ERDF).

References

[1] Cleaner Air - Environment - European Commission, (n.d.). http://ec.europa.eu/environment/air/cleaner_air/ (accessed September 7, 2016).

[2] N. Takahashi, H. Shinjoh, T. Iijima, T. Suzuki, K. Yamazaki, K. Yokota, H. Suzuki, N. Miyoshi, S. Matsumoto, T. Tanizawa, others, The new concept 3-way catalyst for automotive lean-burn engine: NOx storage and reduction catalyst, Catalysis Today. 27 (1996) 63–69.

[3] N. Miyoshi, S. Matsumoto, K. Katoh, T. Tanaka, J. Harada, N. Takahashi, K. Yokota, M. Sugiura, K. Kasahara, Development of New Concept Three-Way Catalyst for Automotive Lean-Burn Engines, in: 1995. doi:10.4271/950809.

[4] B. Guan, R. Zhan, H. Lin, Z. Huang, Review of state of the art technologies of selective catalytic reduction of NOx from diesel engine exhaust, Applied Thermal Engineering. 66 (2014) 395–414. doi:10.1016/j.applthermaleng.2014.02.021.

[5] P. Granger, V.I. Parvulescu, Catalytic NO_x Abatement Systems for Mobile Sources: From Three-Way to Lean Burn after-Treatment Technologies, Chemical Reviews. 111 (2011) 3155–3207. doi:10.1021/cr100168g.

[6] G. Busca, L. Lietti, G. Ramis, F. Berti, Chemical and mechanistic aspects of the selective catalytic reduction of NOx by ammonia over oxide catalysts: A review, Applied Catalysis B: Environmental. 18 (1998) 1–36. doi:10.1016/S0926-3373(98)00040-X.

[7] L. Lietti, G. Ramis, F. Berti, G. Toledo, D. Robba, G. Busca, P. Forzatti, Chemical, structural and mechanistic aspects on NOx SCR over commercial and model oxide catalysts, Catalysis Today. 42 (1998) 101–116.

[8] D.M. Chapman, Behavior of titania-supported vanadia and tungsta SCR catalysts at high temperatures in reactant streams: Tungsten and vanadium oxide and hydroxide vapor pressure reduction by surficial stabilization, Applied Catalysis A: General. 392 (2011) 143–150. doi:10.1016/j.apcata.2010.11.005.

[9] D.M. Chapman, Capture of Volatilized vanadium and tungsten compounds in a selective catalytic reduction system, US 2011/0138789 A1, n.d. (accessed April 27, 2017).
[10] N. Apostolescu, B. Geiger, K. Hizbullah, M.T. Jan, S. Kureti, D. Reichert, F. Schott, W. Weisweiler, Selective catalytic reduction of nitrogen oxides by ammonia on iron oxide catalysts, Applied Catalysis B: Environmental. 62 (2006) 104–114. doi:10.1016/j.apcatb.2005.07.004.
[11] G. Qi, R.T. Yang, Performance and kinetics study for low-temperature SCR of NO with NH_3 over MnO_x–CeO_2 catalyst, Journal of Catalysis. 217 (2003) 434–441. doi:10.1016/S0021-9517(03)00081-2.
[12] Z. Lian, F. Liu, H. He, X. Shi, J. Mo, Z. Wu, Manganese–niobium mixed oxide catalyst for the selective catalytic reduction of NOx with NH_3 at low temperatures, Chemical Engineering Journal. 250 (2014) 390–398. doi:10.1016/j.cej.2014.03.065.
[13] F. Can, S. Berland, S. Royer, X. Courtois, D. Duprez, Composition-Dependent Performance of $Ce_xZr_{1-x}O_2$ Mixed-Oxide-Supported WO_3 Catalysts for the NOx Storage Reduction–Selective Catalytic Reduction Coupled Process, ACS Catal. 3 (2013) 1120–1132. doi:10.1021/cs3008329.
[14] Y. Li, H. Cheng, D. Li, Y. Qin, Y. Xie, S. Wang, WO_3 /CeO_2 -ZrO_2 , a promising catalyst for selective catalytic reduction (SCR) of NOx with NH_3 in diesel exhaust, Chemical Communications. 0 (2008) 1470–1472. doi:10.1039/B717873E.
[15] Z. Ma, D. Weng, X. Wu, Z. Si, Effects of WO_x modification on the activity, adsorption and redox properties of CeO_2 catalyst for NOx reduction with ammonia, Journal of Environmental Sciences. 24 (2012) 1305–1316. doi:10.1016/S1001-0742(11)60925-X.
[16] M. Colombo, I. Nova, E. Tronconi, A comparative study of the NH_3-SCR reactions over a Cu-zeolite and a Fe-zeolite catalyst, Catalysis Today. 151 (2010) 223–230. doi:10.1016/j.cattod.2010.01.010.
[17] P.S. Metkar, M.P. Harold, V. Balakotaiah, Experimental and kinetic modeling study of NH_3-SCR of NOx on Fe-ZSM-5, Cu-chabazite and combined Fe- and Cu-zeolite monolithic catalysts, Chemical Engineering Science. 87 (2013) 51–66. doi:10.1016/j.ces.2012.09.008.
[18] X. Auvray, T. Pingel, E. Olsson, L. Olsson, The effect gas composition during thermal aging on the dispersion and NO oxidation activity over Pt/Al_2O_3 catalysts, Applied Catalysis B: Environmental. 129 (2013) 517–527. doi:10.1016/j.apcatb.2012.10.002.
[19] S. Matsumoto, K. Yokota, H. Doi, M. Kimura, K. Sekizawa, S. Kasahara, Research on new DeNOx catalysts for automotive engines, Catalysis Today. 22 (1994) 127–146. doi:10.1016/0920-5861(94)80097-9.
[20] F. Witzel, G.A. Sill, W.K. Hall, Reaction Studies of the Selective Reduction of NO by Various Hydrocarbons, Journal of Catalysis. 149 (1994) 229–237. doi:10.1006/jcat.1994.1289.
[21] T. Miyadera, Alumina-supported silver catalysts for the selective reduction of nitric oxide with propene and oxygen-containing organic compounds, Applied Catalysis B: Environmental. 2 (1993) 199–205. doi:10.1016/0926-3373(93)80048-I.
[22] A. Flura, F. Can, X. Courtois, S. Royer, D. Duprez, High-surface-area zinc aluminate supported silver catalysts for low-temperature SCR of NO with ethanol, Applied Catalysis B: Environmental. 126 (2012) 275–289. doi:10.1016/j.apcatb.2012.07.006.

[23] P. Kyriienko, N. Popovych, S. Soloviev, S. Orlyk, S. Dzwigaj, Remarkable activity of Ag/Al_2O_3/cordierite catalysts in SCR of NO with ethanol and butanol, Applied Catalysis B: Environmental. 140–141 (2013) 691–699. doi:10.1016/j.apcatb.2013.04.067.

[24] Y.F. Tham, J.-Y. Chen, R.W. Dibble, Development of a detailed surface mechanism for the selective catalytic reduction of NOx with ethanol on silver alumina catalyst, Proceedings of the Combustion Institute. 32 (2009) 2827–2833. doi:10.1016/j.proci.2008.06.190.

[25] S. Sumiya, M. Saito, H. He, Q.-C. Feng, N. Takezawa, K. Yoshida, Reduction of lean NOx by ethanol over Ag/Al_2O_3 catalysts in the presence of H_2O and SO_2, Catalysis Letters. 50 (1998) 87–91.

[26] W.L. Johnson, G.B. Fisher, T.J. Toops, Mechanistic investigation of ethanol SCR of NOx over Ag/Al_2O_3, Catalysis Today. 184 (2012) 166–177. doi:10.1016/j.cattod.2011.12.002.

[27] K. Shimizu, H. Kawabata, A. Satsuma, T. Hattori, Role of Acetate and Nitrates in the Selective Catalytic Reduction of NO by Propene over Alumina Catalyst as Investigated by FTIR, J. Phys. Chem. B. 103 (1999) 5240–5245. doi:10.1021/jp984770x.

[28] K. Shimizu, J. Shibata, H. Yoshida, A. Satsuma, T. Hattori, Silver-alumina catalysts for selective reduction of NO by higher hydrocarbons: structure of active sites and reaction mechanism, Applied Catalysis B: Environmental. 30 (2001) 151–162. doi:10.1016/S0926-3373(00)00229-0.

[29] M. Barreau, M.-L. Tarot, D. Duprez, X. Courtois, F. Can, Remarkable enhancement of the selective catalytic reduction of NO at low temperature by collaborative effect of ethanol and NH_3 over silver supported catalyst, Applied Catalysis B: Environmental. 220 (2018) 19–30. doi:10.1016/j.apcatb.2017.08.015.

[30] M. Richter, R. Fricke, R. Eckelt, Unusual activity enhancement of NO conversion over Ag/Al_2O_3 by using a mixed NH_3/H_2 reductant under lean conditions, Catalysis Letters. 94 (2004) 115–118.

[31] M. Barreau, M. Delporte, E. Iojoiu, X. Courtois, F. Can, Lean NOx Removal by a Bifunctional ($EtOH + NH_3$) Mixture Dedicated to ($Ag/Al_2O_3 + NH_3$-SCR) Dual-Bed Catalytic System: Comparison Between $WO_3/CeZrO_2$ and Cu–FER as NH_3-SCR Catalyst, Top Catal. (2018). doi:10.1007/s11244-018-1104-1.

[32] T.E. Hoost, R.J. Kudla, K.M. Collins, M.S. Chattha, Characterization of Ag/γ-Al_2O_3 catalysts and their lean-NOx properties, Applied Catalysis B: Environmental. 13 (1997) 59–67. doi:10.1016/S0926-3373(96)00090-2.

[33] T. Sato, S. Goto, Q. Tang, S. Yin, DeNOx activity of Ag/γ–Al_2O_3 nanocomposites prepared via the solvothermal route, Journal of Materials Science. 43 (2008) 2247–2253. doi:10.1007/s10853-007-1960-8.

[34] L. Xiaowei, S. Mingmin, H. Xi, Z. Haiyang, G. Fei, K. Yan, D. Lin, C. Yi, Dispersion and Reduction of Copper Oxide Supported on WO_3-Modified $Ce_{0.5}Zr_{0.5}O_2$ Solid Solution, J. Phys. Chem. B. 109 (2005) 3949–3955. doi:10.1021/jp046731t.

[35] A. Musi, P. Massiani, D. Brouri, J.-M. Trichard, P. Da Costa, On the Characterisation of Silver Species for SCR of NOx with Ethanol, Catal Lett. 128 (2009) 25–30. doi:10.1007/s10562-008-9694-z.

[36] M. Seneque, F. Can, D. Duprez, X. Courtois, Use of µ-Scale Synthetic Gas Bench for Direct Comparison of Urea-SCR and NH_3-SCR Reactions over an Oxide Based Powdered Catalyst, Catalysts. 5 (2015) 1535–1553. doi:10.3390/catal5031535.

[37] M. Seneque, F. Can, D. Duprez, X. Courtois, NOx Selective Catalytic Reduction (NO_x-SCR) by Urea: Evidence of the Reactivity of HNCO, Including a Specific Reaction Pathway for NOx Reduction Involving NO + NO_2, ACS Catalysis. 6 (2016) 4064–4067. doi:10.1021/acscatal.6b00785.

[38] C. Ciardelli, I. Nova, E. Tronconi, D. Chatterjee, B. Bandl-Konrad, M. Weibel, B. Krutzsch, Reactivity of NO/NO_2–NH_3 SCR system for diesel exhaust aftertreatment: Identification of the reaction network as a function of temperature and NO_2 feed content, Applied Catalysis B: Environmental. 70 (2007) 80–90. doi:10.1016/j.apcatb.2005.10.041.

[39] M. Iwasaki, H. Shinjoh, A comparative study of "standard", "fast" and "NO_2" SCR reactions over Fe/zeolite catalyst, Applied Catalysis A: General. 390 (2010) 71–77. doi:10.1016/j.apcata.2010.09.034.

[40] Z. Li, B. Šmíd, Y.K. Kim, V. Matolín, B.D. Kay, R. Rousseau, Z. Dohnálek, Alcohol Dehydration on Monooxo W═O and Dioxo O═W═O Species, J. Phys. Chem. Lett. 3 (2012) 2168–2172. doi:10.1021/jz300885v.

[41] C.D. Baertsch, K.T. Komala, Y.-H. Chua, E. Iglesia, Genesis of Brønsted Acid Sites during Dehydration of 2-Butanol on Tungsten Oxide Catalysts, Journal of Catalysis. 205 (2002) 44–57. doi:10.1006/jcat.2001.3426.

[42] R. Allansson, P.G. Blakeman, B.J. Cooper, H. Hess, P.J. Silcock, A.P. Walker, Optimising the Low Temperature Performance and Regeneration Efficiency of the Continuously Regenerating Diesel Particulate Filter (CR-DPF) System, in: 2002. doi:10.4271/2002-01-0428.